Disparity-based Error Concealment for Stereoscopic Images with Superpixel Segmentation

Yizhang Zhang[1], Guijin Tang[1, 2*], Xiaohua Liu[1] and Changming Sun[3]
[1] Jiangsu Key Lab on Image Processing & Image Communication, Nanjing University of Posts and Telecommunications
Nanjing 210003, China
[e-mail: tanggj@njupt.edu.cn]
[2] State Key Laboratory for Novel Software Technology, Nanjing University
Nanjing 210093, China
[3] CSIRO Data61
PO Box 76, Epping, NSW 1710, Australia
*Corresponding author: Guijin Tang

Received October 11, 2017; revised February 16, 2018; accepted April 6, 2018; published September 30, 2018

Abstract

To solve the problem of transmission errors in stereoscopic images, this paper proposes a novel error concealment (EC) method using superpixel segmentation and adaptive disparity selection (SSADS). Our algorithm consists of two steps. The first step is disparity estimation for each pixel in a reference image. In this step, the numbers of superpixel segmentation labels of stereoscopic images are used as a new constraint for disparity matching to reduce the effect of mismatching. The second step is disparity selection for a lost block. In this step, a strategy based on boundary smoothness is proposed to adaptively select the optimal disparity which is used for error concealment. Experimental results demonstrate that compared with other methods, the proposed method has significant advantages in both objective and subjective quality assessment.

Keywords: Superpixel Segmentation, Adaptive Support-Weight, Disparity Estimation, Adaptive Strategy, Disparity Selection

1. Introduction

Due to the wide application prospect in areas of interactive multimedia such as free viewpoint TV and video conference, stereoscopic video technology has attracted increasing attention. However, the compressed bit stream of stereoscopic video is prone to transmission errors [1]. In order to improve the quality of reconstruction image, the error concealment technique, which is only implemented in a decoder and does not need the encoder to provide any additional support or to increase channel cost, has been applied to 3D video transmission.

A few methods have been proposed in the literature. A temporal error concealment algorithm based on moment invariants is presented in [2]. It uses different block sizes which is proportional to the area of each candidate macro-block (MB) for a better feature extraction. Moreover, it utilizes a novel error function based on moment invariants to select the best candidate motion vector. An efficient and highly scalable concealment algorithm for textured color images is introduced in [3]. A lost area is restored by texture extrapolation from the surrounding regions logically associated on the superpixel level. Song et al. [4] developed three concealment modes for the error concealment of multi-view video sequences: temporal bilateral error concealment (TBEC), inter-view bilateral error concealment (IBEC), and multi-hypothesis error concealment (MHEC), and gave a mode selection scheme. An auto-regressive (AR) model based error concealment scheme is proposed for stereoscopic video coding in [5]. The error concealment scheme includes a temporal AR model for independent view, and a temporal-interview AR model for inter-view predicted view. Shadan et al. [6] proposed a new consistency model for error concealment of multi-view plus depth (MVD) video that allows the model to maintain a high level of consistency between frames of the same view (temporal consistency) and those of neighboring views (inter-view consistency). Then they used their model to implement concealment in a consistent manner. A content-adaptive spatial error concealment algorithm is presented in [7]. By using edge information extracted from the surrounding blocks, the error block which has been classified into one of three categories with different contents is reconstructed by appropriate methods to the category it belongs to. A spatial error concealment algorithm for video and images based on convex optimization is proposed in [8]. Missing macroblocks are sequentially reconstructed by filling them with a weighted set of templates extracted from the available neighborhood. A fast-efficient error concealment method for recovering information related to shape is presented in [9]. The proposed technique comprises block classification, edge direction interpolation, and filtering interpolation. A novel spatial error concealment algorithm with an adaptive linear predictor is proposed in [10]. Under the sequential recovery framework, pixels in missing blocks are successively reconstructed based on adaptive linear predictor. Fan et al. [11] proposed an error concealment algorithm based on canonical correlation analysis (CCA). They used CCA to estimate a correlation projection matrix which utilizes the loss of spatial information of macro block adjacent, and then the projection matrix and the adjacent region is used to estimate missing pixel areas. Yang et al. [12] proposed a hybrid error concealment method for slice losses in intra frames of view plus depth stereoscopic video. For lost regions near the edges in the frame, the multi-view (MV) is recovered from the corresponding depth frame. For other regions, the MV is recovered from co-located MB and its neighboring MBs in previous frame. Hu Yang et al.[13] proposed an error concealment scheme, in which the concealment problem is formulated as minimizing, in a weighted manner, the difference between the gradient of the reconstructed data and a

prescribed vector field under given boundary condition. Instead of using the motion compensated block as the final recovered pixel values, they use the gradient of the motion compensated block together with the surrounding correctly decoded pixels of the damaged block to reconstruct the lost data. A concept of motion map that can be easily generated in the decoder side is introduced in [14] and it is combined with the exemplar-based inpainting technique. The proposed method introduces an adaptive search window size that trades-off the quality and complexity. Moreover, an optional blending technique is proposed to limit the spatio-temporal artifacts. The research work in [15] included the spatio-temporal error detection which is combined with different error concealment methods such as copy paste, Block Matching Algorithm and Boundary Matching Algorithm (BMA). The paper presents the comparison of different existing error concealment methods which is combined with spatio temporal error detection. Koloda et al. [16][17] proposed a scalable spatial EC algorithm. The proposed technique exploits the excellent reconstructing abilities of the kernel-based minimum mean square error (K-MMSE) estimator. Error concealment for video coding based on a 3-D discrete wavelet transform (DWT) is considered in [18]. They assumed that the video sequence has a sparse representation in a known basis different from the DWT. Then they formulate the concealment problem as l1–norm minimization and solve it utilizing an iterative thresholding algorithm. The Comparison of different thresholding operators show that Video Block-Matching and 3D filtering provides the best reconstruction by utilizing spatial similarity within a frame and temporal similarity between neighbor frames.

This paper aims to improve the effect of error concealment for stereoscopic images. The contributions of this paper are as follows:

(1) Proposing a disparity estimation strategy using superpixel segmentation to improve the disparity accuracy. Compared with other methods, the proposed strategy can efficiently mitigate the mismatch problem.

(2) Proposing an adaptive disparity selection strategy to select the optimal disparity for a lost block. The proposed adaptive strategy is more flexible and more accurate than traditional disparity selection strategy such as winner-take-all (WTA).

2. Proposed Error Concealment Method

Assume that the left-view image is a damaged image and the right-view image is a correctly decoded image. **Fig. 1** shows the framework of our method. The proposed method is roughly divided into two parts: disparity estimation and disparity selection. Firstly, we segment both left-view image and right-view image of stereoscopic images by a superpixel segmentation method. Then, we estimate disparities by adaptive support-weight matching which uses the superpixel segmentation labels. After that, we utilize the proposed adaptive strategy to select the optimal disparity from the dense disparities. Finally, we use the optimal disparity to extract the data in the right-view image to conceal the damaged block in the left-view image.

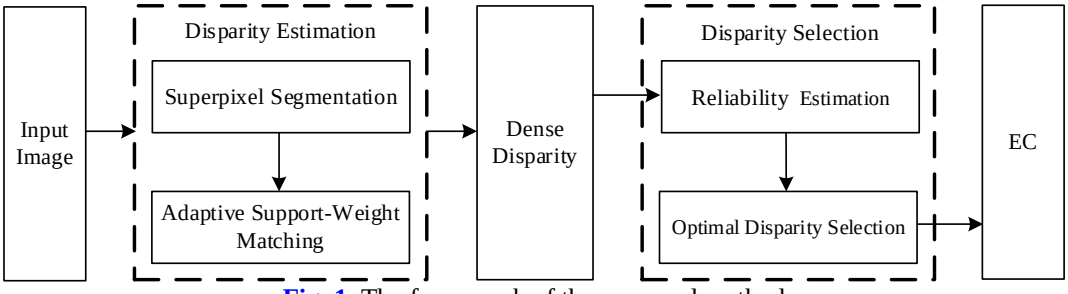

Fig. 1. The framework of the proposed method

2.1 Disparity Estimation with Superpixel Segmentation

According to the different camera positions, three-dimensional imaging system can be divided into parallel structure and rendezvous structure. Stereoscopic images which are acquired by a parallel structure only have horizontal disparities. There are vertical and horizontal disparities in stereoscopic images acquired by a rendezvous structure. However, vertical disparities can be eliminated by stereo image rectification. Therefore, this paper focuses on the stereoscopic images which only have horizontal disparities.

We adopt the block matching method to obtain disparities, which divides an image into macro blocks, then searches their corresponding macro blocks in the reference image for every macro blocks with the assumption of constant disparity inside the macro blocks. The principle of disparity continuity constraint means that the variation of the disparity vector is continuous and smooth except near edge and occlusion areas of an image. According to the above principle, it can be inferred that the disparity of a lost block is the same as the disparities of its adjacent pixels. Therefore, this paper selects the nearest boundary pixels around a lost block as reference pixels to predict the disparity of the lost block.

In order to obtain the dense disparities of above-mentioned pixels, we adopt the window-based matching algorithm. However, if the window whose geometric center is a reference pixel is constructed, it will contain lost pixels. Therefore, for each reference pixel, we design a different base-point-biased window according to its position relative to a lost block, as shown in **Fig. 2**. For more details, we refer the reader to our previous work [19].

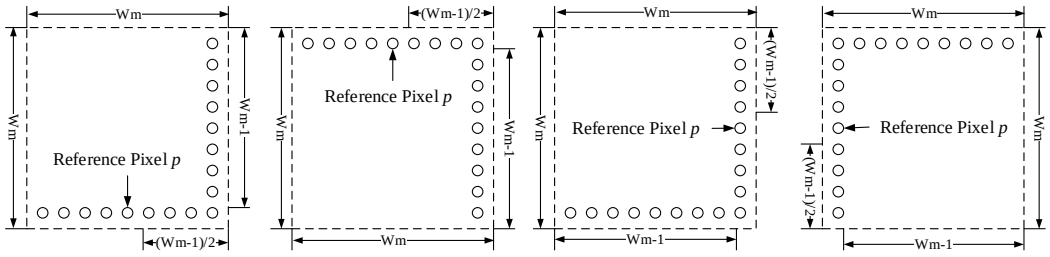

Fig. 2. Reference pixel biased windows

During the search process, the disparity accuracy is undoubtedly the most critical issue. Traditional disparity matching methods only consider the matching cost and ignore the position correlation between pixels. Therefore, they are more likely to result in mismatches.

In order to mitigate the above problem, a disparity estimation with superpixel segmentation in this paper is presented. It uses superpixel segmentation labels as a new constraint for disparity search. Here the Simple Linear Iterative Clustering (SLIC) [20] algorithm is adopted to obtain superpixels.

SLIC algorithm converts the input images from the RGB color space to the CIELAB color space. A pixel's color in the CIELAB color space and its pixel position together compose a five-dimensional data vector used for K-means clustering, i.e.,

$$p_i = [l_i, a_i, b_i, u_i, v_i]^T,\ i = 1, \ldots, M \tag{1}$$

where l_i, a_i and b_i are the luminance component and two color components in the CIELAB color space. u_i and v_i are the positions in the horizontal and vertical directions. Then the SLIC method is implemented using the following measure to obtain the distance between two data vectors.

$$d_{i,j} = \sqrt{(l_i - l_j)^2 + (a_i - a_j)^2 + (b_i - b_j)^2 + \eta\left((u_i - u_j)^2 + (v_i - v_j)^2\right)} \quad (2)$$

where η is designed to control the balance between the color similarity and spatial proximity. When the distances are smaller than a predefined threshold, the corresponding pixels are regarded as belonging to the same class which is defined as a superpixel.

After superpixel segmentation, the number of superpixel label, which is covered by a matching window, is measured. Assume that the numbers of superpixel labels, which are covered by matching windows in the left-view and the right-view images are N_L and N_R respectively. If N_L=N_R, we calculate the matching cost of the current matching. If $N_L \neq N_R$, we conduct the next matching without calculating the matching cost, as shown in **Fig. 3**.

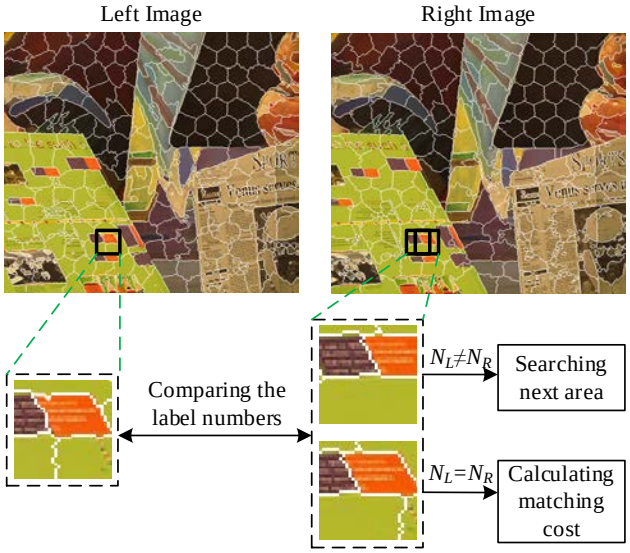

Fig. 3. Search constraint with superpixel segmentation labels

This paper adopts the adaptive support-weight (ASW) disparity matching method [21] to deal with the issue of matching cost calculation. The weight w represents color similarity and geometric position proximity between two pixels

$$w(p,q) = f(\Delta c_{pq}, \Delta g_{pq}) \quad (3)$$

where Δc_{pq} and Δg_{pq} denote the color difference and space distance respectively between pixels p and q. Δc_{pq} and Δg_{pq} can be regarded as independent events [21], so $f(\Delta c_{pq}, \Delta g_{pq})$ is given by

$$f(\Delta c_{pq}, \Delta g_{pq}) = f_s(\Delta c_{pq}) \times f_p(\Delta g_{pq}) \quad (4)$$

And $f_s(\Delta c_{pq})$ and$f_p(\Delta g_{pq})$ and are defined respectively by

$$f_s(\Delta c_{pq}) = exp\left(-\frac{\Delta c_{pq}}{\gamma_c}\right) \quad (5)$$

$$f_p(\Delta g_{pq}) = exp\left(-\frac{\Delta g_{pq}}{\gamma_p}\right) \quad (6)$$

After w is obtained, the matching cost between p and $\bar{p}_d$ is defined by

$$E(p,\bar{p}_d)=\frac{\sum_{q\in N_p,\bar{q}_d\in N_{\bar{p}_d}} w(p,q)w(\bar{p}_d,\bar{q}_d)e(q,\bar{q}_d)}{\sum_{q\in N_p,\bar{q}_d\in N_{\bar{p}_d}} w(p,q)w(\bar{p}_d,\bar{q}_d)} \tag{7}$$

where p and q denote two pixels of the reference image, $\bar{p}_d$ and $\bar{q}_d$ are the corresponding pixels of the target image and d is the disparity between p and$\bar{p}_d$. N_p and $N_{\bar{p}_d}$ denote the window whose biased reference pixels are p and$\bar{p}_d$. e (q,$\bar{q}_d$) is the matching cost between q and$\bar{q}_d$. For each target pixel, we choose the disparity which can satisfy the minimum $E(p,\bar{p}_d)$ as its optimal disparity, namely

$$d_p = arg\,min_{d\in S_d} E(p,\bar{p}_d) \tag{8}$$

We perform this operation for all reference pixels around a lost block, and therefore obtain local dense disparities D= $\{d_p\}$ of the lost block.

2.2 Adaptive Strategy for Optimal Disparity Selection

After obtaining local dense disparities, a disparity should be selected for the lost block. Next the image data will be extracted from the reference image according to this disparity of the lost block to conceal the missing pixels.

Because of occlusion, uniform and/or, repetitive regions, the estimated disparity may not be reliable. Therefore, local dense disparities are checked using the consistency constraint in our method,

$$R'(x,y)=\begin{cases}1, & |d_{LR}(x,y)+d_{RL}(x',y)|\le T\\ 0, & otherwise\end{cases} \tag{9}$$

where $d_{LR}(x,y)$ and $d_{RL}(x',y)$ denote the disparity of pixel (x, y) from the left-view image to the right-view image and the disparity of pixel (x', y) from the right-view image to the left-view image respectively, and T is a threshold. We conduct this operation on all local dense disparities, and obtain a reliable disparity set.

Next we will select a disparity from the reliable disparity set as the disparity of a lost block. Because the disparities in the reliable disparity set varies, a common method for selection is WTA. However, WTA do not work well if the neighboring content of a lost block changes. In this paper, we propose an adaptive strategy to select the optimal disparity of a lost block. This strategy has higher accuracy than the traditional WTA strategy.

Sorting the disparities D in descending order according to the frequency of all elements. We define that the disparity of the N_i pixels is D_{Ni}. Then we obtain the disparities set D_r= $\{D_{Ni}\}$, (i=*1, 2,* ⋯) from D. The disparity value of D_r is unique. N is the total number of pixels which have reliable disparities. We can define that the number N_i of pixels whose reliable disparity is D_{Ni} accounted for the proportion of N as

$$R_i = N_i/N \tag{10}$$

We set a threshold P_T and obtain P_j as follows (j=*1, 2,* ⋯)

$$P_j = \sum_{i=1}^{j} R_i \tag{11}$$

We collect the disparities whose corresponding R_j or N_i satisfy the conditions $P_j<P_T$ and $N_i \neq 1$. These collected disparities D_{Ni} ($i=1, 2, \cdots, j$).become the candidates of the optimal disparity, namely D_{cand}. Then we use every element in D_{cand} to try to conceal the lost block, and calculate the smoothness of the boundary between the recovered result of the lost block and its surrounding pixels (as shown in **Fig. 4**). We use the sum of squared difference (SSD) as the evaluation metric to calculate the boundary smoothness, i.e.

$$\begin{aligned} BoundarySSD = & \sum_{x=x_1}^{x_1+s-1}[p(x,y_1-1)-p(x,y_1)]^2 \\ & +\sum_{x=x_1}^{x_1+s-1}[p(x,y_1+s-1)-p(x,y_1+s)]^2 \\ & +\sum_{y=y_1}^{y_1+s-1}[p(x_1-1,y)-p(x_1,y)]^2 \\ & +\sum_{y=y_1}^{y_1+s-1}[p(x_1+s-1,y)-p(x_1+s,y)]^2 \end{aligned} \quad (12)$$

where s is the size of a lost block.

Finally, we select the disparity whose SSD is minimum as the optimal disparity D_{opt}, and then use D_{opt} to extract the data to conceal the lost block.

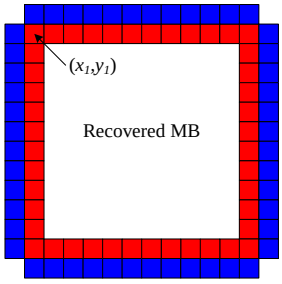

Fig. 4. Illustration of the external and internal boundary of a recovered MB

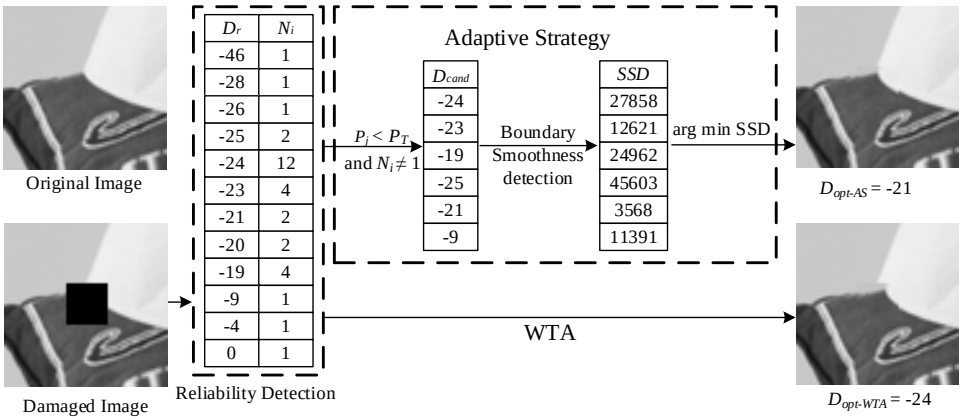

Fig. 5. The adaptive strategy for selecting the optimal disparity

As an example, **Fig. 5** shows the difference between our adaptive selection strategy and WTA. The steps for the optimal disparity selection are summarized in **Algorithm1**.

Algorithm 1 Selecting Optimal Disparity

- **Input**: local dense disparity
- Reliability detection: obtain reliable disparity set
- Adaptive selection:
  - Reliable disparity ranking
  - for i=1:reliable disparity number
    $R_i = N_i/N$; $R = R + R_i$;
    if P_j>=P_T or N_i =1 break; end
    end
  - for m=1:i
    Error concealment using the candidate disparity and selecting optimal disparity;
    end
- **Output**: the optimal disparity

3. Experimental Results

In order to test the effect of the proposed method, we conduct a series of simulation experiments. Objective and subjective quality assessment is used as the indicator of the performance of our method.

We use the peak signal to noise ratio (PSNR) and Structural similarity (SSIM) as the objective measure, and choose stereoscopic image *Teddy*, *Tsukuba*, *Cones*, *Baby1*, *Baby3*, *Books*, *Dolls*, *Moebius*, *Monopoly*, and *Rocks1* [22]as the test images, as shown in **Fig. 6**. The number of superpixels is set to 3500 and the P_T is set to 0.7 experimentally. The block-loss ratio γ is set to 5%, 10%, and 15% in our experiments. We compare the performance of our method with zero vector method (ZV), Kernel-Based MMSE (KMMSE)[17], XFSE[23], weighted template matching (WTM) [8], and auto-regressive model based error concealment (AR) [5].

In order to test the effectiveness of our proposed adaptive disparity selection strategy, we also carried out the following experiments. We combine our proposed disparity estimation strategy with the WTA strategy into a test error concealment method called SSADS-1. As shown in **Table 1**, the best result is highlighted in each cell.

Fig. 6. Test images

Table 1 and **Table 2** have shown that compared with other methods, both the proposed disparity estimation method and the adaptive strategy for selecting optimal disparity has achieved noticeable improvements. The PSNR of our method is more than 1 dB higher than other methods for most test images. For the stereoscopic images of *cloth1*, our method even has the advantages of more than 3 dB in PSNR. Compared with other methods, the SSIM value

of our method also has advantage.

We also calculate the average PSNR and SSIM of each EC method for all test images, as shown in the AVE column of **Table 1** and **Table 2**. The average PSNR data are shown in **Fig. 7**. It is clear that the performance of our proposed algorithm is much better than other error concealment algorithm in the cases of higher γ.

For large size image processing, processing time is a very important index. Here we take image *baby3* for example. We expand it to the size of 1920*1080 and measure the execution time when different algorithms conceal its losing blocks, as shown in **Table 3**. The block-loss ratio γ is set to 5%. In view of the PSNR and SSIM of our method, its execution time is acceptable.

Table 1. Comparison of objective quality of error concealment methods in terms of PSNR (dB)

	teddy	tsukuba	cones	baby1	baby3	books	dolls	midd2	moebius	rocks1	AVE
	γ≈5%										
ZV	25.12	26.92	26.44	34.76	26.63	23.37	30.10	24.76	25.55	27.93	27.16
KMMSE	34.09	34.30	33.62	41.49	36.14	34.93	34.56	**42.69**	37.50	35.80	36.51
XFSE	34.95	33.59	33.33	41.22	35.71	**35.94**	34.74	38.24	37.71	35.39	36.08
WTM	33.43	33.26	32.92	41.10	35.62	33.35	34.98	36.29	35.29	35.24	35.15
AR	37.64	35.85	34.20	41.16	36.96	34.19	40.42	36.80	36.34	38.33	37.19
SSADS-1	34.43	35.96	33.61	41.79	37.75	35.18	34.12	36.58	36.21	37.65	36.33
SSADS	**37.96**	**37.37**	**34.37**	**42.58**	**38.15**	35.69	**40.59**	40.53	**37.86**	**38.48**	**38.36**
	γ≈10%										
ZV	21.90	25.61	22.50	30.73	25.46	21.20	26.80	23.05	23.83	26.10	24.72
KMMSE	33.49	30.74	30.68	37.95	36.50	32.18	29.79	34.34	34.49	33.75	33.39
XFSE	33.71	31.37	30.46	38.09	35.57	33.35	30.33	33.63	33.81	33.11	33.34
WTM	33.30	30.65	30.21	38.27	36.14	33.38	31.37	32.64	34.30	33.92	33.42
AR	29.50	33.08	29.45	32.52	29.89	27.82	34.48	29.86	30.90	31.64	30.92
SSADS-1	29.10	32.26	29.75	**40.00**	35.21	36.04	31.48	31.43	34.60	36.70	33.66
SSADS	**34.04**	**36.17**	**31.50**	39.84	**38.72**	**36.07**	**36.97**	**35.02**	**35.97**	**37.53**	**36.18**
	γ≈15%										
ZV	21.00	24.97	21.61	28.87	23.47	20.14	25.57	22.65	23.09	23.13	23.45
KMMSE	30.38	29.81	29.46	34.68	33.85	29.91	28.31	32.78	33.52	31.72	31.44
XFSE	30.49	30.28	29.26	34.90	33.07	30.90	28.65	31.71	32.73	31.11	31.31
WTM	29.86	29.31	29.07	35.72	33.24	29.98	30.64	32.33	33.52	31.67	31.53
AR	28.58	30.49	28.34	29.91	28.65	26.72	33.00	29.23	29.50	30.55	29.50
SSADS-1	28.17	31.78	28.78	36.47	32.98	34.15	28.65	30.91	33.54	35.02	32.05
SSADS	**32.25**	**35.17**	**30.29**	**37.32**	**36.34**	**34.65**	**35.26**	**34.51**	**35.00**	**35.82**	**34.66**

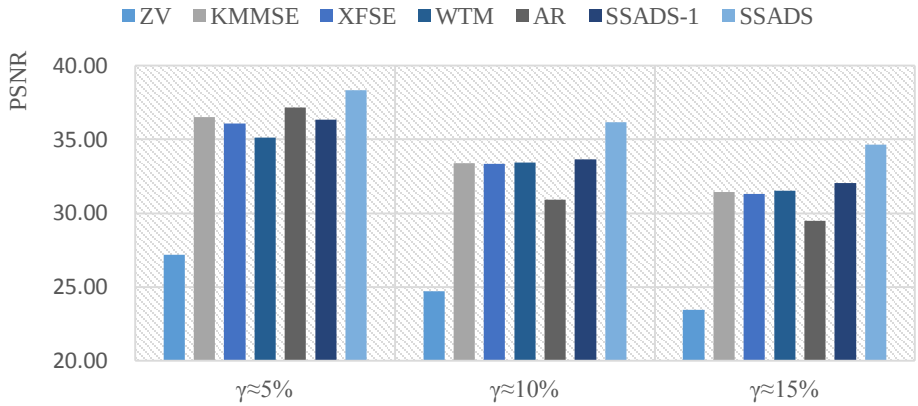

Fig. 7. Comparison of EC methods in average PSNR (dB)

Table 2. Comparison of objective quality of error concealment methods in terms of SSIM (scaled by 100)

	teddy	tsukuba	cones	baby1	baby3	books	dolls	midd2	moebius	rocks1	AVE
	$\gamma\approx5\%$										
ZV	92.70	94.70	91.66	96.07	93.03	92.28	91.77	94.90	91.78	93.94	93.28
KMMSE	97.48	98.01	96.62	98.47	98.18	98.79	97.47	99.69	**98.45**	97.36	98.05
XFSE	97.37	97.50	96.08	98.29	97.96	98.55	97.36	99.42	98.36	97.29	97.82
WTM	97.36	97.86	96.49	98.40	98.12	98.62	97.36	99.61	98.30	97.33	97.95
AR	**98.79**	98.59	**97.91**	98.74	**98.56**	98.56	97.92	99.28	98.03	**98.71**	98.51
SSADS	98.63	**98.73**	97.63	**98.93**	98.52	**98.83**	**97.96**	**99.45**	98.28	98.45	**98.54**
	$\gamma\approx10\%$										
ZV	87.50	91.72	85.66	92.22	88.73	87.97	87.23	92.82	86.74	89.03	88.96
KMMSE	96.39	96.36	94.00	96.81	97.33	97.82	95.08	98.89	96.93	96.13	96.57
XFSE	96.12	95.88	93.39	96.68	96.97	97.33	94.54	98.32	96.55	95.66	96.14
WTM	96.29	95.98	93.89	96.89	97.14	94.97	94.97	98.67	96.85	96.17	96.18
AR	95.33	97.12	94.78	94.97	94.38	94.23	95.11	95.78	95.85	95.98	95.35
SSADS	**97.59**	**98.14**	**95.94**	**98.15**	**97.93**	**98.36**	**96.92**	**98.94**	**97.87**	**98.11**	**97.80**
	$\gamma\approx15\%$										
ZV	82.08	89.19	78.97	86.69	81.75	81.95	77.89	89.22	80.91	81.70	83.04
KMMSE	94.02	94.85	91.64	93.76	95.35	95.71	92.49	97.96	95.43	93.19	94.44
XFSE	93.45	94.23	90.73	93.64	94.78	94.91	91.42	97.11	94.68	92.58	93.75
WTM	93.81	94.47	91.51	93.85	95.04	95.24	92.29	97.72	95.18	93.19	94.23
AR	93.40	96.40	91.92	92.52	92.56	92.23	92.89	93.67	93.32	94.18	93.31
SSADS	**96.28**	**97.83**	**94.01**	**97.10**	**97.03**	**97.61**	**95.24**	**98.57**	**96.97**	**96.91**	**96.76**

Table 3. Comparison of the processing time of error concealment methods for image *baby3* (s)

ZV	KMMSE	XFSE	WTM	AR	SSADS
8.2731	7727.9033	160.8160	1453.5562	11.7240	794.0262

We then compare the subjective quality assessment of above methods. Here we take *Midd2*, *Tsukuba*, *Teddy* as examples as given in **Figs. 8-10**. It can be observed that our method has achieved excellent performance in many areas such as those marked by red rectangles.

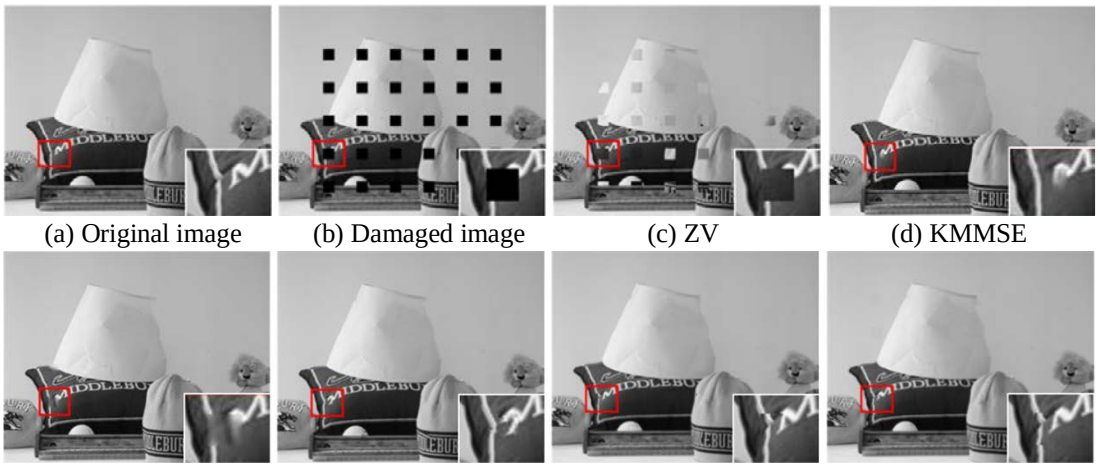

(a) Original image (b) Damaged image (c) ZV (d) KMMSE

(e)XFSE (f) WTM (g) AR (h) SSADS

Fig. 8. Comparison of subjective quality on image *Midd2* ($\gamma \approx 5\%$)

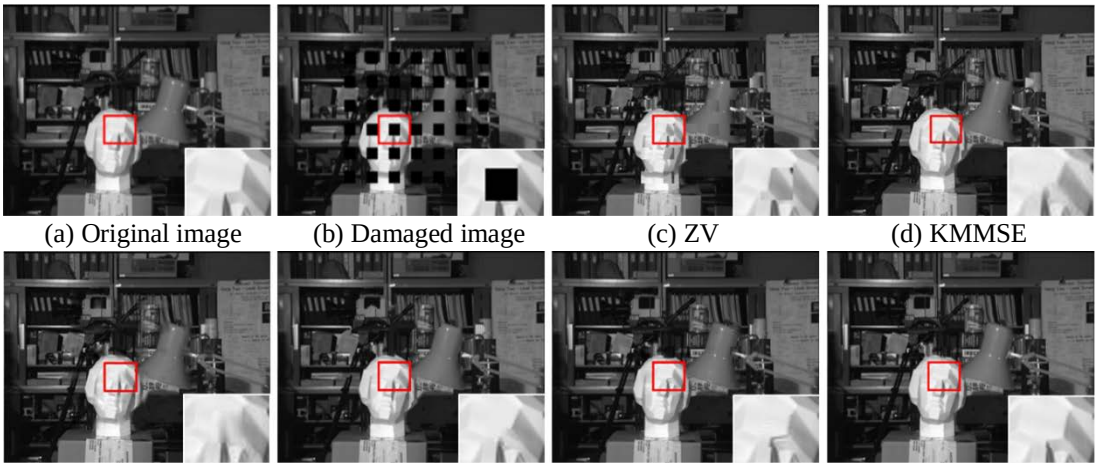

(a) Original image (b) Damaged image (c) ZV (d) KMMSE

(e) XFSE (f) WTM (g) AR (h) SSADS

Fig. 9. Comparison of subjective quality on image *Tsukuba* ($\gamma \approx 10\%$)

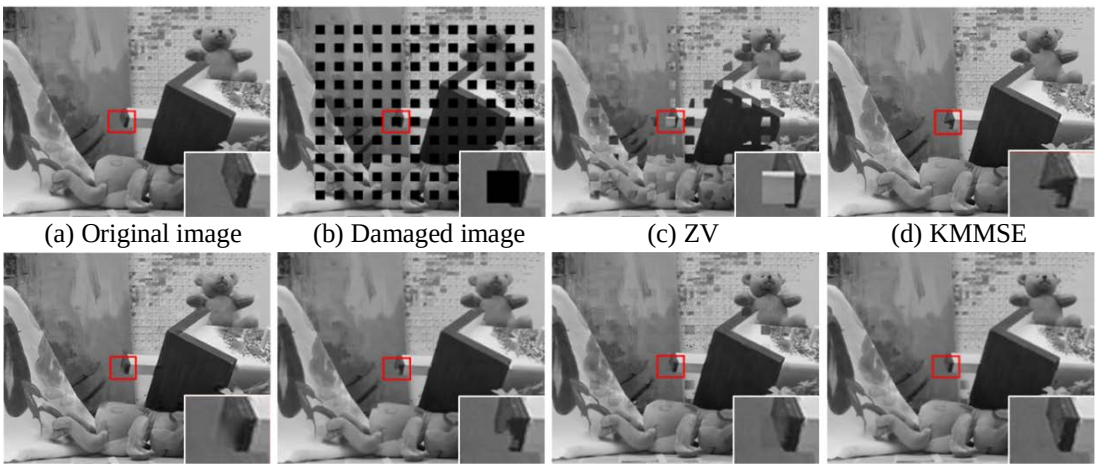

(a) Original image (b) Damaged image (c) ZV (d) KMMSE

(e)XFSE (f) WTM (g) AR (h) SSADS

Fig. 10. Comparison of subjective quality on image *Teddy* ($\gamma \approx 15\%$)

4. Conclusions

This paper proposes a novel error concealment method using superpixel segmentation and adaptive disparity selection. In the process of disparity estimation, we segment images using the superpixel segmentation method. Then we add a new constraint for disparity search using the superpixel segmentation labels. After obtaining the local dense disparities and handling them with reliability detection, we adopt our proposed adaptive strategy to select the optimal disparity which is used for accurate error concealment from reliable disparity set. Experimental results demonstrate that compared with other methods, the proposed method can achieve significant improvements on both quantitative measure and visual assessment.

References

[1] Liang, Yi J., John G. Apostolopoulos, and Bernd Girod. "Analysis of packet loss for compressed video: Effect of burst losses and correlation between error frames," *IEEE Transactions on Circuits and Systems for Video Technology* 18.7, 861-874, 2008. Article (CrossRef Link)

[2] Marvasti-Zadeh, Seyed Mojtaba, Hossein Ghanei-Yakhdan, and Shohreh Kasaei. "A novel video temporal error concealment algorithm based on moment invariants," in *Proc. of Machine Vision and Image Processing (MVIP), 2015 9th Iranian Conference on*. IEEE, 2015. Article (CrossRef Link)

[3] Ilčíková, Ivana, et al. "Texture aware image error concealment with fuzzy segmentation," *Systems, Signals and Image Processing (IWSSIP), 2016 International Conference on*. IEEE, 2016. Article (CrossRef Link)

[4] Song, Kwanwoong, et al. "Error concealment of multi-view video sequences using inter-view and intra-view correlations," *Journal of Visual Communication and Image Representation* 20.4, 281-292, 2009. Article (CrossRef Link)

[5] Xiang, Xinguang, et al. "Auto-regressive model based error concealment scheme for stereoscopic video coding," in *Proc. of Acoustics, Speech and Signal Processing (ICASSP), 2011 IEEE International Conference on*. IEEE, 2011. Article (CrossRef Link)

[6] Khattak, Shadan, et al. "Temporal and inter-view consistent error concealment technique for multiview plus depth video," *IEEE Transactions on Circuits and Systems for Video Technology* 26.5, 829-840, 2016. Article (CrossRef Link)

[7] Rongfu, Zhang, Zhou Yuanhua, and Huang Xiaodong. "Content-adaptive spatial error concealment for video communication," *IEEE Transactions on Consumer Electronics* 50.1, 335-341, 2004.Article (CrossRef Link)

[8] Østergaard, Jan, et al. "Sequential error concealment for video/images by weighted template matching," *Data Compression Conference (DCC)*, IEEE, 2012. Article (CrossRef Link)

[9] Hsia, Shih-Chang, and Cheng Hung Hsiao. "Fast-efficient shape error concealment technique based on block classification," *IET Image Processing* 10.10, 693-700, 2006. Article (CrossRef Link)

[10] Liu, Jing, et al. "Spatial error concealment with an adaptive linear predictor," *IEEE Transactions on Circuits and Systems for Video Technology*, 25.3, 353-366, 2015. Article (CrossRef Link)

[11] Fan, Wen, et al. "Sequential error concealment via canonical correlation analysis," in *Proc. of Signal Processing, Communications and Computing (ICSPCC), 2015 IEEE International Conference on*. IEEE, 2015. Article (CrossRef Link)

[12] Yang, Yuhong, Meng Yang, and Pamela Cosman. "A hybrid error concealment for intra frame in stereoscopic video," *Signal Processing Conference (EUSIPCO), 2012 Proceedings of the 20th European*. IEEE, 2012. Article (CrossRef Link)

[13] Hu, Yang, et al. "An improved spatio-temporal video error concealment algorithm using partial differential equation,"*Proceedings of SPIE, the International Society for Optical Engineering*. Society of Photo-Optical Instrumentation Engineers, 2005. Article (CrossRef Link)

[14] Aldahdooh, Ahmed, et al. "Inpainting-based error concealment for low-delay video communication," in *Proc. of Acoustics, Speech and Signal Processing (ICASSP), 2017 IEEE International Conference on*. IEEE, 2017. Article (CrossRef Link)
[15] Pathak, Ketki C., Shubhi Singh, and Jigisha N. Patel. "Error detection and concealment algorithm for compressed video transmission," in *Proc. of Humanitarian Technology Conference (R10-HTC), 2016 IEEE Region 10*. IEEE, 2016. Article (CrossRef Link)
[16] Koloda, Ján, et al. "Scalable kernel-based minimum mean square error estimator for accelerated image error concealment,"*IEEE Transactions on Broadcasting* 63.1, 59-70, 2017. Article (CrossRef Link)
[17] Koloda, Ján, et al. " Kernel-Based MMSE Multimedia Signal Reconstruction and Its Application to Spatial Error Concealment,"IEEE *Transactions on Multimedia*, 16.6, 1729-1738, 2014. Article (CrossRef Link)
[18] Belyaev, Evgeny, Soren Forchhammer, and Marian Codreanu. "Error concealment for 3-D DWT based video codec using iterative thresholding," *IEEE Communications Letters*, 2017. Article (CrossRef Link)
[19] Tang, Gui-Jin, Xiu-Chang Zhu, and Tian-Liang Liu. "An error concealment algorithm for stereoscopic images based on local reliable disparities," *Dianzi Xuebao (Acta Electronica Sinica)*, 41.4, 781-786, 2013. Article (CrossRef Link)
[20] Achanta, Radhakrishna, et al. "SLIC superpixels compared to state-of-the-art superpixel methods," *IEEE transactions on pattern analysis and machine intelligence*, 34.11, 2274-2282, 2012. Article (CrossRef Link)
[21] Yoon, Kuk-Jin, and In So Kweon. "Adaptive support-weight approach for correspondence search," *IEEE Transactions on Pattern Analysis and Machine Intelligence*, 28.4, 650-656, 2006. Article (CrossRef Link)
[22] http://vision.middlebury.edu/stereo/data/
[23] Koloda J, Seiler J, Kaup A, et al. "Frequency selective extrapolation with residual filtering for image error concealment," in *Proc. of Acoustics, Speech and Signal Processing (ICASSP), 2014 IEEE International Conference on*. IEEE, 2014. Article (CrossRef Link)

Yizhang Zhang received his BE degree from the Jinling Institute of Technology (JIT), Nanjing, China, in 2014, in Communication engineering (CE). He is currently working toward his ME degree in Signal and information processing (SIP) from Nanjing University of Posts and Telecommunications (NJUPT). His research interests include image processing and error concealment.

Guijin Tang received his Ph.D. degree in signal and information processing from Nanjing University of Posts and Telecommunications, Nanjing, Jiangsu, China, in 2013. He is currently an Associate Professor at Nanjing University of Posts and Telecommunications, Nanjing, China. His research interests include image and video coding, and image restoration.

Xiaohua Liu is currently pursuing her Ph.D. degree with the School of Electronic Science and Engineering, Nanjing University of Posts and Telecommunications, China. Her research interests include image processing, pattern recognition, and machine learning.

Changming Sun received his PhD degree in computer vision from Imperial College London, London, UK in 1992. He then joined CSIRO, Sydney, NSW, Australia, where he is currently a Principal Research Scientist carrying out research and working on applied projects. His current research interests include computer vision, image analysis, and pattern recognition. He has served on the program/organizing committees of various international conferences. He is an Associate Editor of the EURASIP Journal on Image and Video Processing. He is a member of the Australian Pattern Recognition Society.